INDEPENDENT VERIFICATION AND VALIDATION OF ARTEMIS I ASCENT INTEGRATED FLIGHT PERFORMANCE SIMULATIONS

Jacob Fleck,[*] Tannen VanZwieten Cook,[†] John Davidson,[‡] Ivan Bertaska,[§] Jeremy Shidner,[‖] and Charlie Hall[#]

The NASA Engineering and Safety Center (NESC) has performed independent model development to support cross-model verification for the Space Launch System (SLS) Program since 2012 which culminated, for Artemis I, in a postflight reconciliation analysis of the Artemis I ascent trajectory (validation). This post-flight analysis was completed by both the NESC and the SLS Program. Upon successful completion of the Artemis I mission, multiple preflight simulations of the nominal ascent trajectory were updated with Day of Launch (DOL) conditions and simulated results were compared to reconstructed flight data derived from telemetry measurements. Dispersed trajectories were also produced using a combination of DOL conditions and preflight uncertainties, which ideally should bound the Artemis I flight data. Finally, multibody dynamics were simulated for some of the separation events to support clearance analyses. This paper focuses on validating and understanding the accuracy of the models by comparing simulated results against the Artemis I flight data. In addition, discrepancies uncovered between simulations led to opportunities to investigate areas for potential model improvement to refine preflight simulations for future Artemis missions. Included in this paper is background on the flight performance simulation tools, the postflight analysis approach, and a comparison of simulation results against the Artemis I flight data. Simulated results were found to generally be in close agreement with each other and the Artemis I flight data.

INTRODUCTION

NASA successfully flew the Artemis I mission on November 16, 2022, marking the inaugural flight of the Space Launch System (SLS). A decade prior to this, the NASA Engineering and

[*] Aerospace Engineer, Atmospheric Flight and Entry Systems Branch, Analytical Mechanics Associates, NASA Langley Research Center, Hampton, VA, 23681, USA.
[†] Assoc. Principal Engineer, NASA Engineering and Safety Center, Kennedy Space Center, FL, USA.
[‡] Aerospace Engineer, Dynamic Systems & Control Branch, NASA Langley Research Center, Hampton, VA, 23681, USA.
[§] Team Lead, Control Systems Design & Analysis Branch, NASA Marshall Space Flight Center, Huntsville, AL, 35812, USA.
[‖] Aerospace Engineer, Atmospheric Flight and Entry Systems Branch, NASA Langley Research Center, Hampton, VA, 23681, USA
[#] Aerospace Engineer, Control Systems Design & Analysis Branch, Axient Corp, NASA Marshall Space Flight Center, Huntsville, AL, 35812, USA.

Safety Center (NESC)* assembled a dedicated team of subject matter experts, independent from the SLS Program (SLSP), to develop an end-to-end simulation of the Artemis I SLS ascent trajectory and to perform detailed analyses of critical separation events. The NESC has continually supported the Artemis Program by performing Independent Verification and Validation (IV&V) analyses and by providing expertise to support technical integration and mitigate risks between the Artemis Programs: the Space Launch System Program (SLSP), the Multi-Purpose Crew Vehicle Program (MPCVP), and the Exploration Ground Systems Program (EGSP). Throughout the SLSP design cycle, the NESC has performed independent, ascent trajectory simulations to evaluate Space Launch System (SLS) integrated performance and separation clearance assessments using computational tools separate from the SLSP. With each analysis, NESC results were compared to SLSP results and any NESC findings or observations were reported to the SLSP. In addition to the value-added through IV&V, having an independent integrated simulation that was mature and verified ensured that the NESC could leverage this capability to rapidly address potential issues throughout the program lifecycle by avoiding the long lead times typically associated with the development of a complex flight simulation.

Artemis I launched from Complex 39B at NASA Kennedy Space Center (KSC) in Florida on Wednesday, November 16, 2022, at 1:47am EST and completed its mission on December 11 with splashdown of the Orion Capsule in the Pacific Ocean. Data from the Artemis I mission was used to validate the NESC and SLSP trajectory simulation tools, which remain in use for the analysis of flight and separation performance for future crewed Artemis missions. This provided the opportunity to better understand the current level of simulation accuracy, to disposition any modeling errors between simulations, and to identify areas of model improvement prior to future SLSP analyses. To accomplish these goals, each modeling and simulation team performed a postflight reconciliation, which involved updating preflight trajectory simulations with Day of Launch (DOL) flight conditions for comparison against the reconstructed Artemis I trajectory data. The following sections introduce the flight performance simulation models and tools used by the NESC and the SLSP, discuss the postflight analysis approach, and provide a qualitative understanding of the data products and associated results.

Flight Performance Simulation Tools

Throughout the SLSP design cycle, simulations were used by each independent modeling and simulation team to produce preflight, point-mass, dynamic simulations of the SLS ascent trajectory. Nominal preflight trajectories were produced by Marshall Aerospace Vehicle Representation in C (MAVERIC),[5] a TREETOPS†-derived tool called CLVTOPS,[2] Space Transportation & Aeronautics Research Simulation (STARS),[4] and Program to Optimize Simulated Trajectories II (POST2),[6] which were compared against each other for IV&V purposes. In addition to comparing nominal trajectories, dispersed trajectories were produced by a subset of these simulation tools to evaluate flight scenarios with varied model parameters. Finally, the results of these preflight dispersed trajectories were used in conjunction with discretized vehicle geometries and additional computational tools to compute minimum clearances between various geometries of interest dur-

*The NESC was established by NASA after the Space Shuttle Columbia accident of 2003. It serves as an independent, Agency-wide engineering resource that performs assessments of its high-risk projects to ensure safety and mission success.[3]

† The name TREETOPS refers to the class of structures which may be simulated by the program, i.e., those having a tree topology (where loop closures are handled with a cut graph technique) (NASA Technology Transfer Program Design and Integration Tools: https://software.nasa.gov/software/MFS-33566-1).

ing a variety of multibody separation events. A summary of the trajectory simulation tools can be found in Table 1.

Table 1. Flight Performance Simulation Tools

Tool	NASA Center	Language	Domain
MAVERIC	Marshall	C/C++	Time
CLVTOPS	Marshall	FORTRAN Python	Time
STARS	Langley	MATLAB Simulink	Time Frequency
POST2	Langley	C	Time

In addition to the trajectory simulation tools listed, other trajectory software tools have been used to model the Artemis I ascent, but this paper will focus on the software tools listed as they were used for the postflight analysis. The postflight comparison was also a collaborative effort across multiple different teams and organizations, but the results and observations presented are from the perspective of the POST2 modeling and simulation team and additional context is provided regarding the POST2 results compared to the other simulations.

Postflight Analysis Approach

The postflight reconciliation followed a process similar to preflight performance analyses. Simulation runs performed in MAVERIC, CLVTOPS, STARS, and POST2 were updated with DOL flight conditions, and each tool produced a nominal ascent trajectory. Dispersed trajectories were produced and evaluated by the respective modeling and simulation teams but, for this multi-simulation comparison 2,000 dispersed trajectories were generated with POST2 using Monte Carlo Techniques. Any models or datasets that could not be represented using DOL data products defaulted to using the most recent preflight engineering models. A list of data products that were used to update the nominal POST2 simulation to DOL conditions can be found in Table 2.

Table 2. Artemis I DOL Models Implemented into POST2

Model	Artemis I DOL Update
Aerodynamics	Reconstructed Base Force Profile
Solid Rocket Booster Performance	Reconstructed Booster Thrust Profile
Core Stage Engine Performance	Postflight Core Engine Parameters
Mass Properties	Reconstructed Mass Properties
GN&C	DOL GN&C Inputs
Atmosphere & Winds	Measured DOL Atmospheric & Wind Conditions

For the dispersed cases, POST2 relied primarily on preflight engineering dispersions and uncertainty models. One of the few notable exceptions however was that optimized open-loop steering inputs were not generated for each dispersed POST2 trajectory. As a result, only the DOL open-loop steering inputs were utilized for all dispersed cases.

The postflight simulations produced by MAVERIC, CLVTOPS, STARS, and POST2 were compared against each other and against Artemis I reconstructed flight data derived from telemetry measurements. Additionally, in some instances, raw telemetry measurements were compared against simulated measurements as well. Together, the reconstructed flight data and telemetry measurements were considered the Best Estimate of Trajectory (BET) of the Artemis I vehicle's performance for the purpose of this reconciliation. For a complete list of data products used in this analysis including simulated results, DOL inputs, and BET results, see Appendix A.

A primary goal of this comparison effort was for each modeling and simulation team to refine their simulation tools by identifying any simulation outliers and discrepancies in preparation for future SLSP analyses. Therefore, the nominal DOL simulated trajectories produced by MAVERIC, CLVTOPS, STARS, and POST2 were qualitatively compared against each other and against the BET. Any differences in initial conditions or simulated trends between the nominal simulations were further diagnosed. Furthermore, the CLVTOPS and POST2 simulations were later used to drive postflight separation and clearance analyses.[6] Although the separation analyses themselves are not the emphasis of the present paper, the matching of flight performance simulations was a prerequisite before conducting postflight separation and clearance analyses. For more information on the NESC Artemis I postflight separation and recontact analyses along with information regarding additional tools used for this analysis, please see *Independent Verification and Validation of Artemis I Separation Events*.[7] Another goal of this analyses was to observe if the Artemis I BET was bounded by the POST2 dispersed trajectories. Flight data outside the Monte Carlo bounds suggests a real flight scenario beyond simulation predictions, which could indicate an issue with the simulation's ability to predict the vehicle performance, or an unanticipated issue during flight. would indicate an issue with the simulation's ability to predict the vehicle performance, or an unanticipated issue during flight. Identifying and assessing these outliers helps inform about limitations in existing models, data, or dispersions especially in situations where the BET and nominal DOL simulations may disagree. Finally, successful completion of this work was expected to provide confidence in the tools' accuracy and capabilities in advance of future SLSP analyses.

RESULTS

The results provided in the following sections are a small subset of results from the complete NESC Artemis I postflight investigation and comparison effort.[8] The subset of results selected for this paper focus on differences that were observed between the simulated results and the BET as well as observed differences across simulations. Most data products showed high levels of agreement between simulation results and the BET and were thus omitted from this paper. Any observed differences in initial conditions or simulated trends between the nominal simulations were further diagnosed. Most simulation artifacts that were uncovered by this comparison were resolved by the modeling and simulation teams, and some were identified as areas for potential future model development.

Trajectory Parameters – Position & Velocity

Figures 1 and 2 compare the vehicle's true earth-relative position and velocity, respectively, to the that of the BET. The vehicle translational states are in good agreement across simulations and are bounded by the POST2 dispersed trajectories. These two figures are examples of desired re-

sults where the nominal trajectory results from the individual tools and the BET are overlapping and are also bounded by the POST2 dispersed trajectory results. However, note that in Figure 1, the altitude is biased towards the upper bound of the Monte Carlo mid-trajectory shortly after Launch Abort System (LAS) Jettison. This observation and potential contributing factors will be discussed further in subsequent sections.

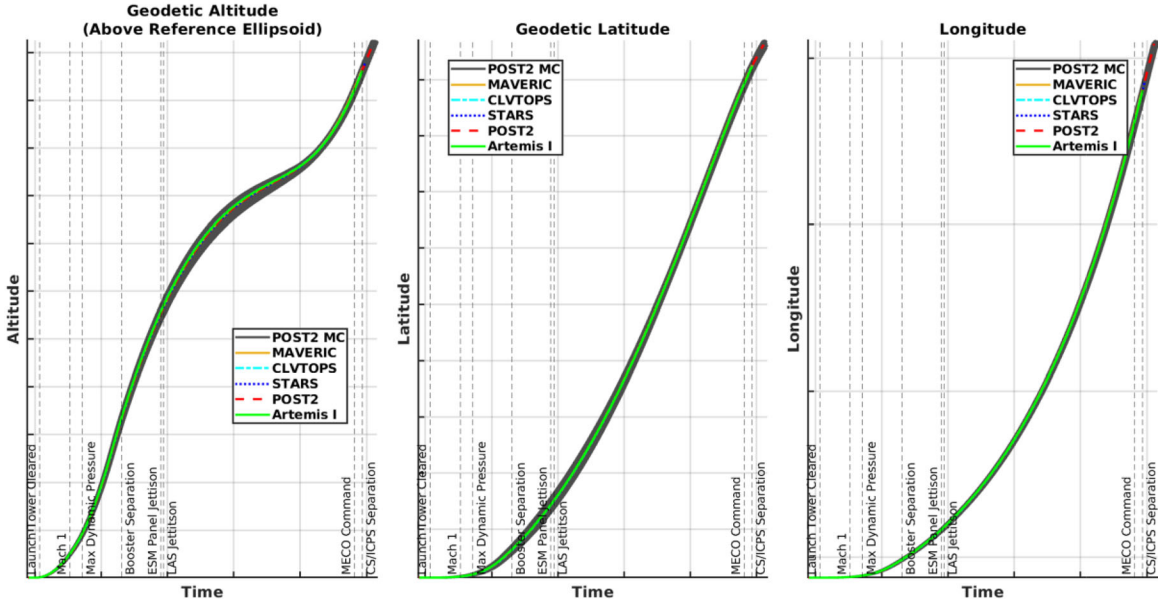

Figure 1. Earth-Relative Position

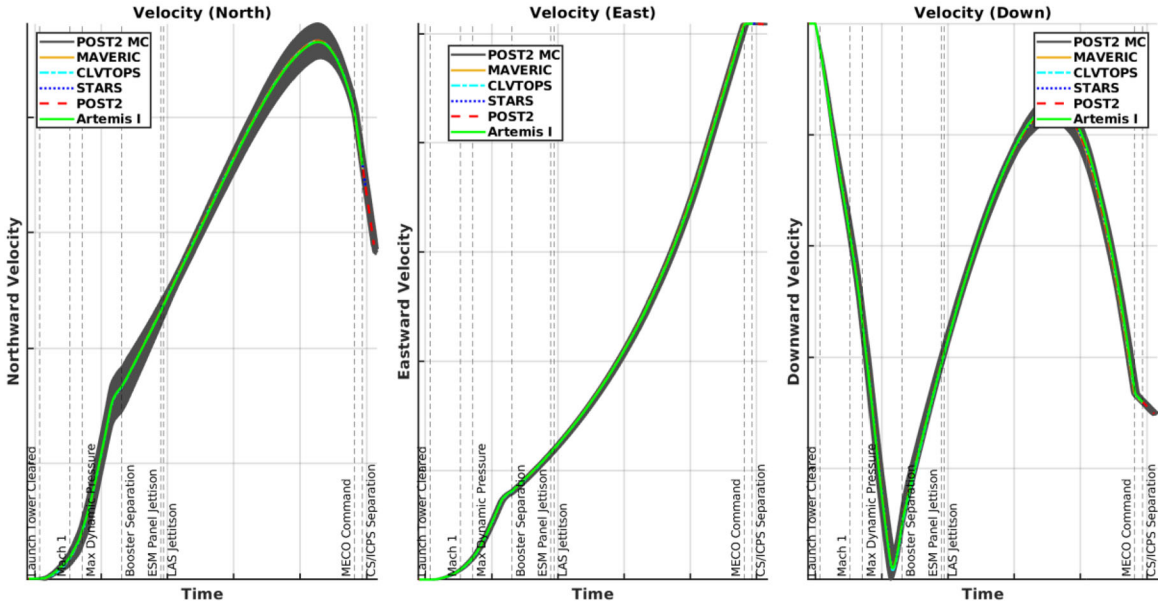

Figure 2. Earth-Relative Velocity

Trajectory Parameters – Body Accelerations

The simulated and reconstructed nominal body accelerations shown in Figure 3 are in good agreement across simulations and were generally well-bounded by the POST2 dispersed trajecto-

ries. However, the Artemis I reconstruction shows a small bias that was not observed in simulations along the vehicle y-axis. It was also noted that the Artemis I y-axis body acceleration extends just beyond the bounds of the POST2 Monte Carlo profiles prior to Main Engine Cutoff (MECO). Similarly, a visible bias was observed along the z-axis, but the z-axis accelerations were still mostly bounded by the Monte Carlo results.

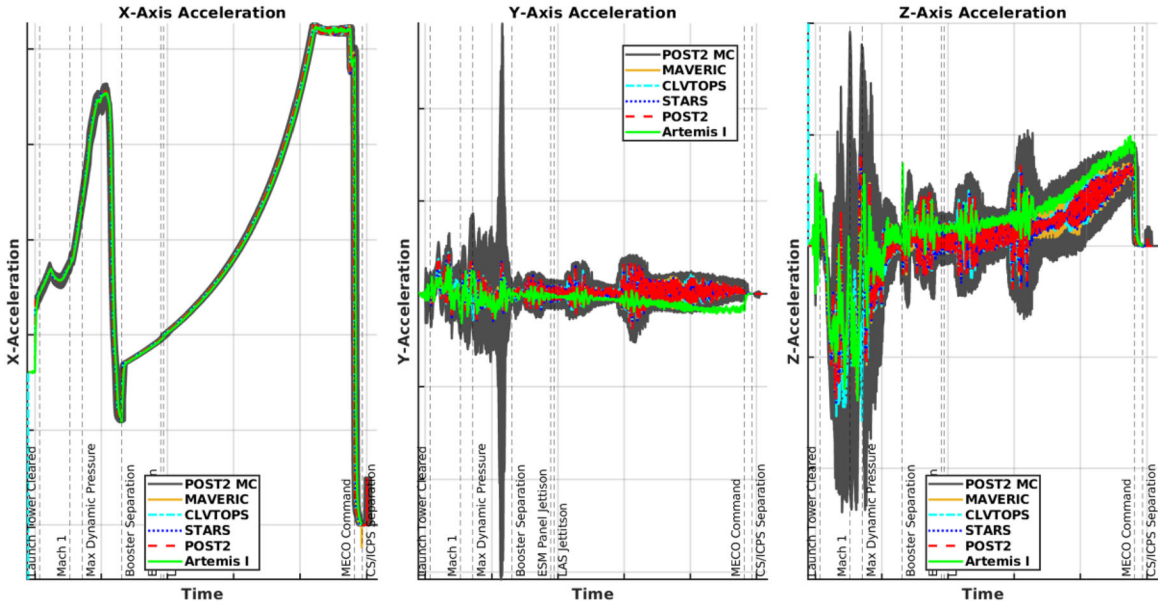

Figure 3. Vehicle Body Accelerations (Sensed – Excluding Gravity)

Potential causes for the observed biases along the y- and z-axes were considered. First, because the Artemis I accelerations in Figure 3 were reconstructed from telemetry measurements, it is possible that the accelerometer measurements were noisier and more biased than anticipated by the manufacturer and/or the steady state bias was not sufficiently filtered out during the reconstruction process. Secondly, the Artemis I reconstructed accelerations along the y-axis appear to further stray from the simulated results after LAS separation. It is possible, though unlikely, that the LAS separation event could have negatively impacted an Artemis I accelerometer's performance. For example, the sensor could have sustained a hardware issue resulting from LAS separation such as physical damage or a sudden change in temperature, both of which could have negatively impacted the accelerometer's performance. In addition to hardware issues, mounting misalignment was also considered, which can be a contributor to steady state bias. The POST2 Monte Carlo simulation disperses mounting misalignments of accelerometers therefore, either the mounting misalignment dispersion method requires updating or mounting misalignment was not the correct culprit. Finally, the Artemis I accelerometers could have been detecting acceleration contributions from un-modeled dynamics (aerodynamic, vibrational, slosh affects, etc.) during this flight regime. Although this flight data was beyond simulation predictions, the magnitude of these accelerations was small compared to the vehicle's total mass and therefore the overall flight performance of Artemis I was considered unaffected by this observation.

Trajectory Parameters – Mach Number & Dynamic Pressure

Figure 4 compares Mach number and dynamic pressure. The Artemis I dynamic pressure agreed with the nominal, simulated results. Additionally, the time at which Artemis I experienced maximum dynamic pressure was also aligned with the simulated maximum dynamic pressure time in all cases. However, differences were observed in the Mach number results for POST2.

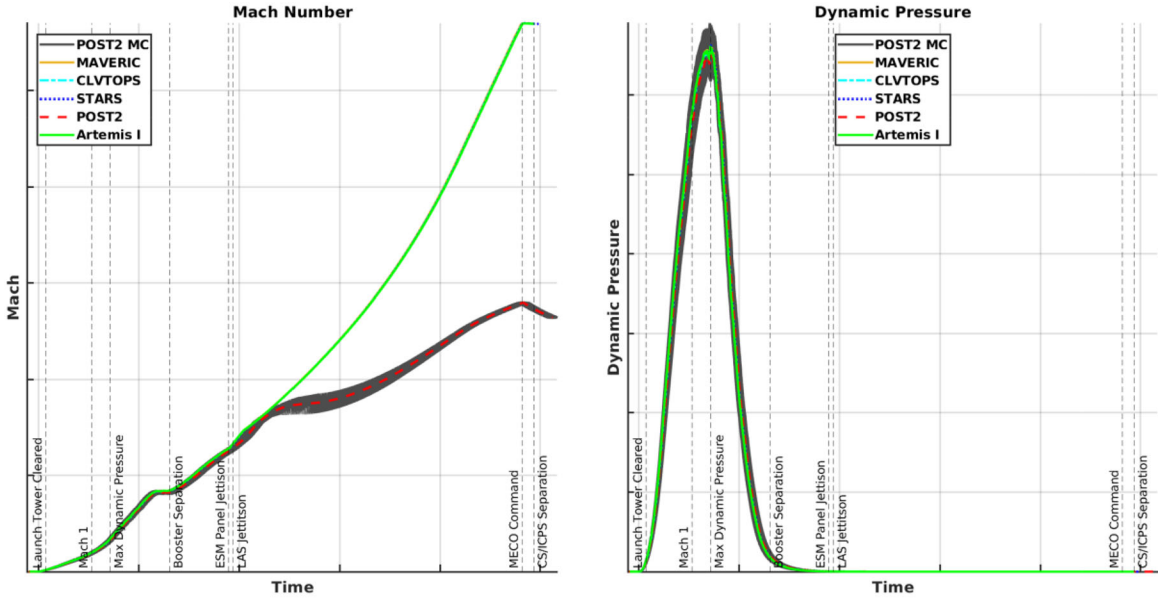

Figure 4. Mach Number and Dynamic Pressure

It was determined that the differences in the POST2 Mach number were due to POST2 computing the speed of sound at upper altitudes whereas other simulations and data sources assumed a constant value. Around this point in the trajectory, the vehicle flies through the rarified flow regime, which drives this assumption. Figure 5 shows updated results for Mach number where POST2 has adjusted its simulation to implement the same assumption regarding the speed of sound in air to align with the other simulations and the BET. This adjustment was purely for consistency across simulations as it minimally impacted the POST2 results. While flying through the rarified flow regime, SLS experiences minimal dynamic pressure, and thus minimal aerodynamic forces. Therefore, the simulated dynamics are unaffected despite the change in Mach number.

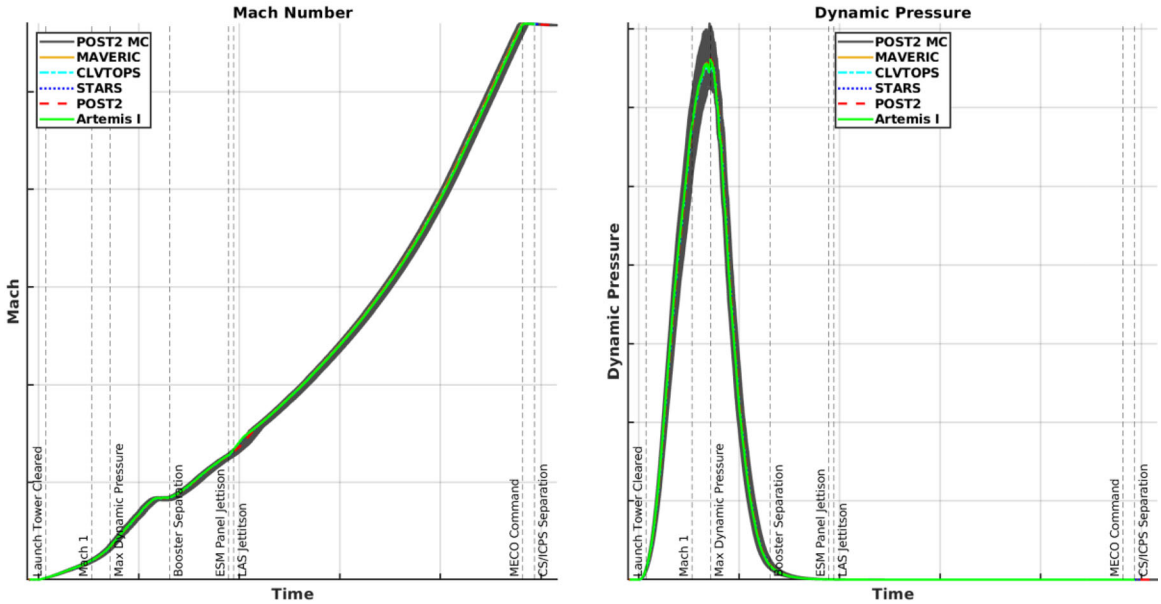

Figure 5. Corrected Mach Number and Dynamic Pressure

Geodetic Altitude – Simulation Initialization

Figure 6 shows the vehicle's altitude at the beginning of the simulation while the vehicle is still located on the launchpad. It is a zoomed-in view of the vehicle's altitude from Figure 1 without the POST2 dispersed trajectories present. The left-hand plot shows that MAVERIC and CLVTOPS agree while POST2 and STARS are also in agreement but at a lower altitude. Meanwhile, the reconstructed altitude lies between the two sets of agreeing simulations but is located closer to MAVERIC and CLVTOPS.

The right-hand plot in Figure 6 shows the same datasets except the POST2 nominal trajectory was re-evaluated with its slosh model turned off. When turning the slosh model off in POST2, it was observed that POST2 reported a higher altitude prior to liftoff while the vehicle was still at rest on the launchpad, which is indicated by the POST2 results now lying between the BET and STARS results. This indicates a change in the vehicle's location simply by turning off the POST2 slosh model. POST2 refers to the location of the vehicle's center of gravity when computing altitude thus, turning on and off the slosh model more accurately indicates a change in the center of gravity location.

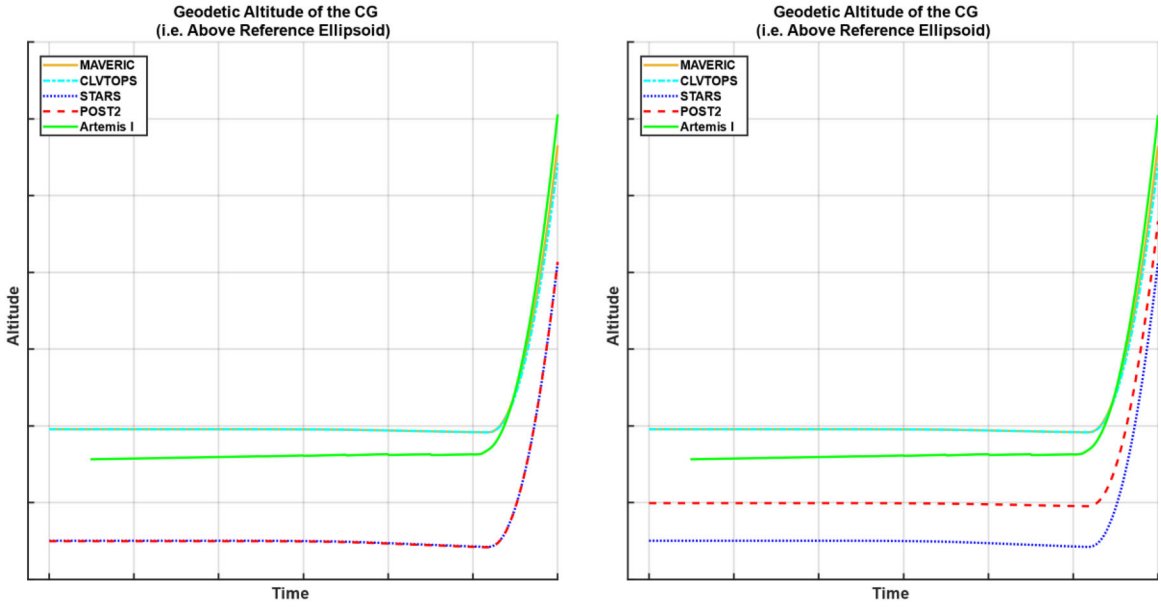

Figure 6. Geodetic Altitude at Simulation Initialization (Launchpad)

The slosh model formulation in POST2 requires all designated sloshing masses to be removed from the fully integrated vehicle, which are then given their own respective equations of motion. Any forces and moments produced by the slosh model were then treated as external forces and moments acting on the remaining vehicle. After slosh mass removal, the remaining vehicle mass properties are recomputed and referred to as the effective mass properties. Thus, the plots in Figure 6 indicate that POST2 and STARS reference the effective center of gravity location on the vehicle when computing altitude rather than referencing the center of gravity of the fully integrated vehicle.

In addition to offsets from slosh model affects, this comparison also revealed that POST2 and STARS needed to update the initial height above the reference ellipse, which accounted for the remaining offset between simulations. For future SLS comparisons, the POST2 team updated the

model outputs to report altitude with respect to the fully integrated vehicle center of gravity location to align with MAVERIC and CLVTOPS (improved results not shown).

Finally, it was observed that none of the simulations fully agreed with the reconstruction at initialization. This may have been due to variation in the mass property dataset when generating the reconstruction. This would result in a slightly different center of gravity location between the simulations and reconstruction when computing altitude. Differences in reconstructed mass property datasets are discussed in further detail in the subsection titled "Mass Properties". Before the corrections were made by the POST and STARS teams, the differences in simulation results were well within one vehicle length and the adjustments reduced this further. These differences were found to have little impact on the overall simulation results. Instead, this comparison illustrates the level of detail that was considered and the refinement of simulation tools to mitigate differences prior to future SLS analyses.

Geodetic Altitude – Mid Trajectory

Figure 7 shows a zoomed-in view of the vehicle's altitude mid-trajectory shortly after LAS Jettison. Despite being bounded by the Monte Carlo results, differences in the magnitude of the vehicle's altitude appeared significant upon first inspection when comparing the nominal simulations to the BET. Figure 7 shows that the BET is biased towards the high end of the Monte Carlo results and that CLVTOPS maintains the closest match to the BET during this time. Meanwhile, the remaining simulations reported a consistently lower altitude than the BET. However, despite these differences, Table 3 shows that the percent difference in altitude between the simulations and the BET is less than half of a percent.

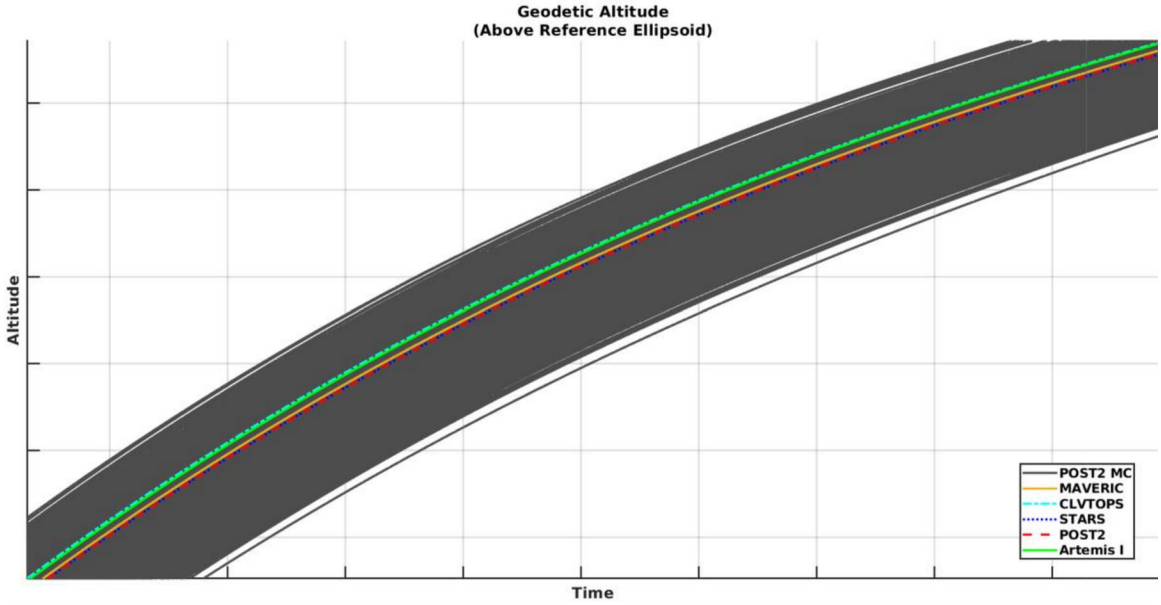

Figure 7. Geodetic Altitude Mid-Trajectory

Table 3. Percent Difference of Simulated Altitude from BET

Model	Percent Difference
CLVTOPS	0.045
MAVERIC	-0.26
POST2	-0.37
STARS	-0.38

Potential causes for the small differences in altitude include vehicle mass variations, propellant mass flow rate, and timing/synchronization across simulations. It is expected that differences in the simulated mass properties (discussed in more detail in the "Mass Properties" subsection) will result in different vehicle states and therefore, different altitude. Additionally, subsection "Mass Properties – Mass Flow Rate" explains that differences in the simulated propellant mass flow rate was also observed across simulations, which will cause further differences in the simulated vehicle mass properties and vehicle thrust throughout the trajectory, both of which will impact the vehicle's altitude profile. Additionally, the rate of change of altitude was large mid-trajectory due to the vehicle's high speed. Thus, any small differences in timing and synchronization across the simulations had the ability to report seemingly large differences in altitude. Therefore, any small differences in timing and synchronization across the simulations would result in relatively large differences in the reported altitude.

Vehicle Attitude – Quaternion

The vehicle attitude quaternion, shown in Figure 10, was in good agreement across the simulations.

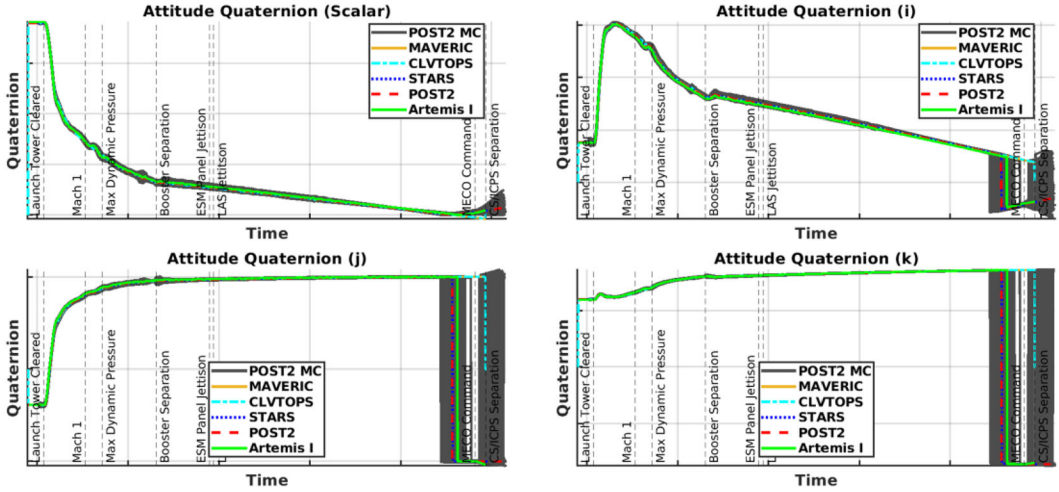

Figure 10. Inertial Frame to Body Frame Attitude Quaternion

The reconstructed quaternion had to be post-processed to perform this comparison. The BET provided the EMEJ2000 to vehicle body frame attitude quaternion time history, but not all the simulations track or report results with respect to the EMEJ2000 inertial frame. Thus, the reconstruct-

ed EMEJ2000 quaternion was post-processed using the information data system known as the Spacecraft, Planet, Instrument, C-matrix, Events (SPICE)[1] to reflect an estimate of the simulated Inertial Frame to the Vehicle Body Frame quaternion.

Vehicle Attitude – Rates and Accelerations

Figure 11 plots the vehicle attitude rates, and Figure 12 shows the angular accelerations. The vehicle attitude rates and accelerations agreed well across the simulations except for the vehicle roll rate.

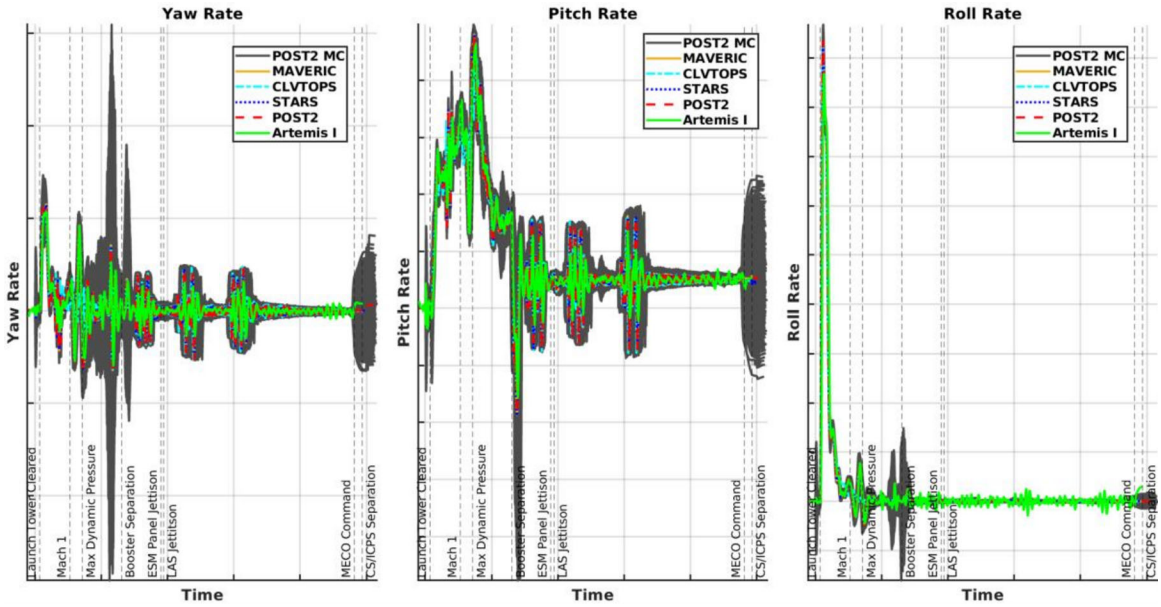

Figure 11. Attitude Rates about Body Frame Axes

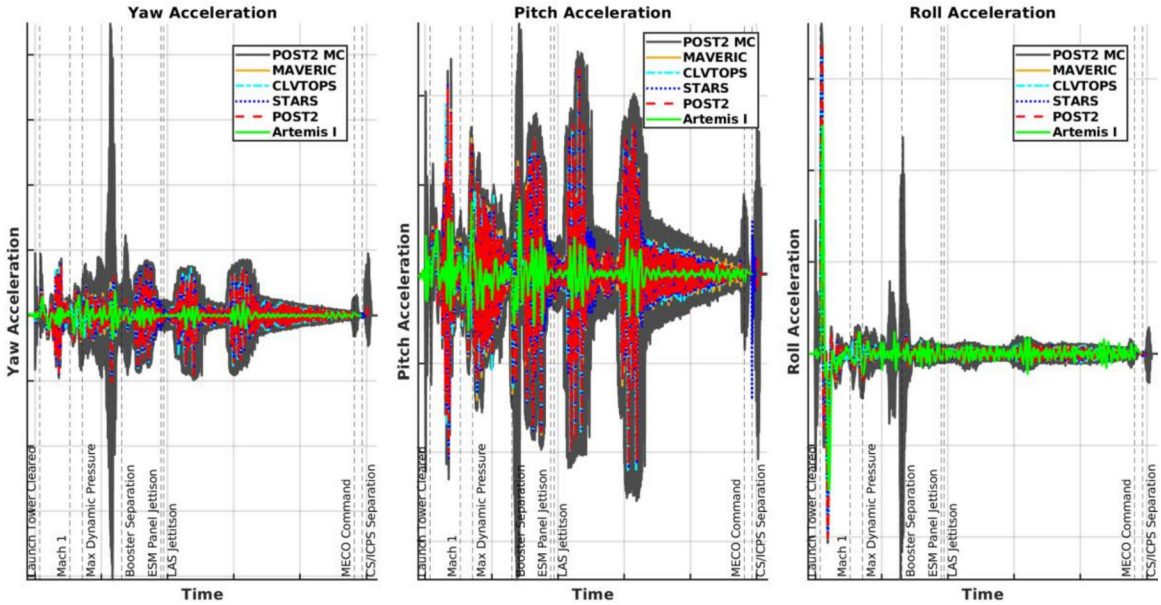

Figure 12. Angular Accelerations about Body Frame Axes

The simulated dispersed vehicle roll rate profiles did not bound the Artemis I reconstructed roll rate between jettison of the LAS and MECO. The simulated, core stage engine gimbal friction model fidelity may require additional updating to capture the physics of the flight hardware more accurately despite previous modeling efforts. An update to this model may sufficiently degrade the simulated gimbal performance causing the simulated results to better represent the BET. The SLSP has been working to update this model to better simulate the behavior of the flight hardware.

Additionally, Figure 13 shows a zoomed-in view of the roll rate and the rolling angular acceleration immediately after the launch tower has been cleared. Immediately after tower clearance, Artemis I performs a roll maneuver and Figure 13 shows that the simulated results overperform the maneuver compared to the BET.

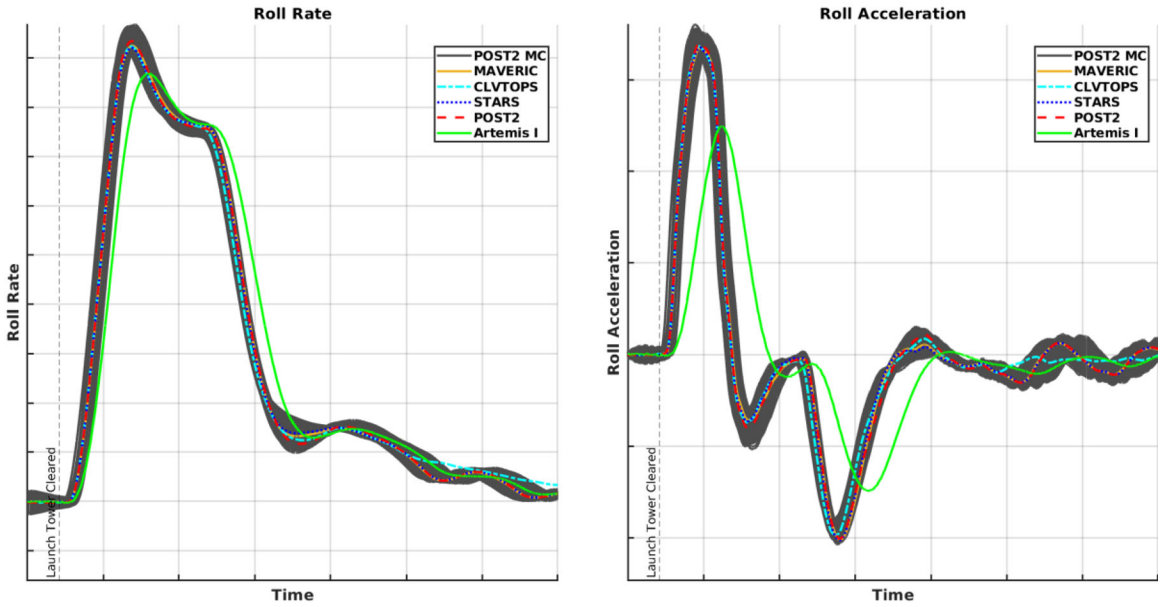

Figure 13. Tower Clearance Roll Maneuver Performance

The largest amount of error observed between the BET and the POST2 nominal trajectory during this time is approximately 10%. The simulated results show that the maximum roll rate and roll acceleration achieved is greater than that of the Artemis I BET. The simulated results then converge faster on the desired equilibrium roll-state concluding the maneuver. Prior to Solid Rocket Booster (SRB) separation, the booster Thrust Vector Control (TVC) system has a majority of the control authority. Therefore, it was originally thought that updates to the simulated booster TVC system would degrade the performance of the simulated results thereby decreasing the maximum roll rate and roll acceleration achieved while also increasing the equilibrium convergence time. These changes would cause the simulated results to be in phase with the BET. However, the SLSP team that produced the BET results confirmed after the comparisons were conducted that the telemetry measurements were low pass filtered to eliminate measurement noise. This introduced a delay in the roll channel and reduce the maximum roll rate observed in the BET during this maneuver. Therefore, the observed mismatch between the BET and the simulation results was likely driven by the filtering that was done to reduce noise the measurement noise.

Additionally, recall that dispersed open-loop steering inputs were not generated for the POST2 Monte Carlo analysis. Had dispersed steering inputs been generated, the expectation is that the bounds of the Monte Carlo for the attitude, angular rates, and angular accelerations would be

wider prior to SRB separation since each trajectory would follow its own unique steering inputs rather than the nominal steering inputs. Thus, the dispersed POST2 results would envelope more variations in the BET prior to SRB separation. The comparison in Figure 13 was found to be the greatest source of percent error between the simulated results and the BET.

Mass Properties

For the postflight mass property analysis, two different postflight mass property data products were generated for Artemis I using separate computational tools. These two mass property datasets were generated to serve separate purposes. First, the BET mass properties dataset contains a time-history of change in the vehicle mass properties. This dataset is the slightly more accurate version of the two datasets and is considered the best estimate of the Artemis I mass properties throughout the vehicle's ascent. Second is the DOL initial rollout mass properties. Unlike the BET mass properties, the DOL initial rollout mass properties only contain the vehicle's mass properties prior to liftoff. This dataset is intended to be used as initial conditions for dynamic simulation purposes and is considered less accurate than the BET mass properties due to different assumptions in model formulation. Because these two mass property reconstructions were produced with different tools and to serve two different purposes, the two resulting datasets are expected to have minor differences between them regarding the initial vehicle mass properties.

Vehicle mass is presented in Figure 14 from liftoff to MPCV/ICPS separation. The vehicle masses agree, and separation events appear to be synchronized except for the separation of the Interim Cryogenic Propulsion Stage (ICPS) modeled in POST2. This comparison revealed that the timer for trigging ICPS separation in POST2 required updating. Additional minor differences in vehicle mass were observed in the initial vehicle mass and the simulated propellant mass consumption rate, which are shown in Figure 15 and Figure 16 respectively.

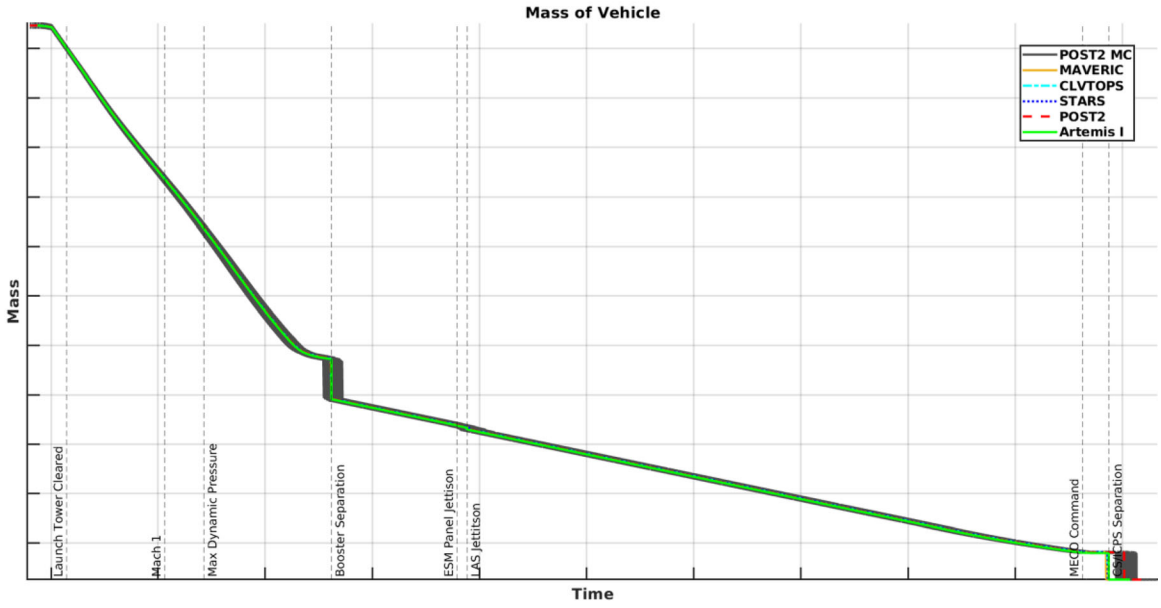

Figure 14. Artemis I Vehicle Mass

Mass Properties – Initial Vehicle Mass

Figure 15 shows the initial mass of the vehicle prior to launch. Notice that the mass properties of the Artemis I BET does not reflect the same start time as the other datasets. It was assumed that the Artemis I BET mass properties were constant prior to its initial datapoint.

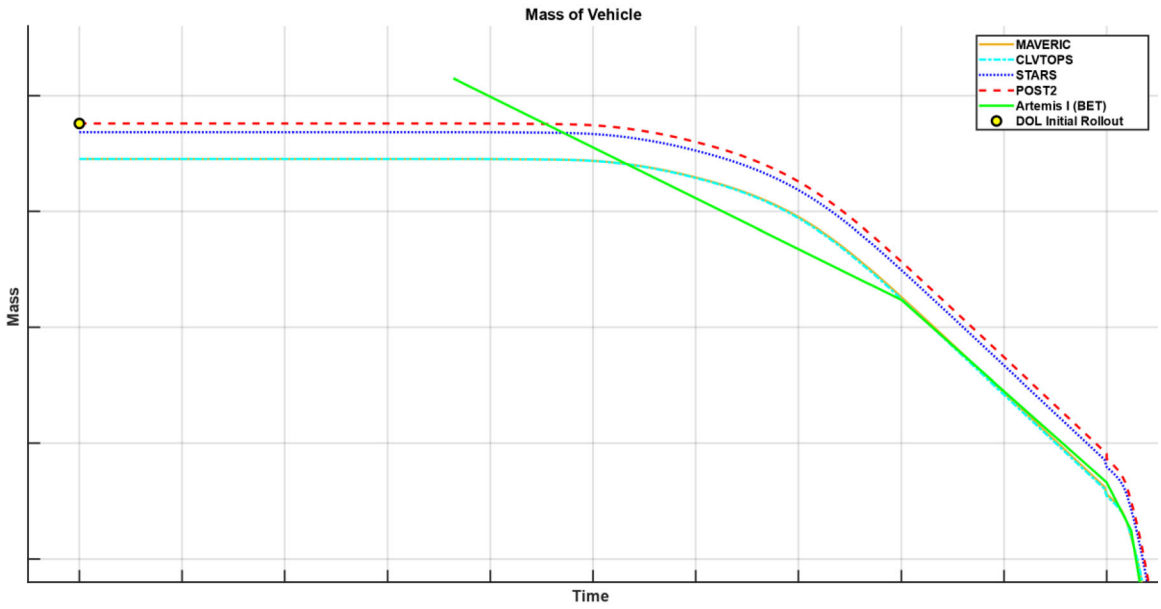

Figure 15. Initial Vehicle Mass

The MAVERIC and CLVTOPS simulations appeared to be missing a small amount of initial mass compared to the DOL initial rollout vehicle mass. STARS also reported slightly lower mass than the DOL initial rollout vehicle mass. A small amount of numerical error between the DOL initial rollout vehicle mass and the initial simulated vehicle mass properties is expected due interpolating fuel tank table data provided by the DOL initial rollout mass properties. However, the remaining error in initial vehicle mass was undetermined. During this analysis, multiple versions of the DOL initial rollout mass properties were produced and therefore it is possible that different simulations had implemented different versions of this dataset at the time this analysis was performed. Nonetheless, when compared to the vehicle's total mass of over 5 million pounds, the amount of missing mass is relatively small and had little impact on performance (as seen by the previous figures).

Mass Properties – Propellant Mass Flow Rate

Figure 16 displays the simulated vehicle mass error over time. This comparison assumes that the BET vehicle mass is the true vehicle mass (i.e., Artemis I BET has zero error). Positive error indicates that the simulated mass is greater than the BET and negative error indicates the simulation is less massive than the BET. Thus, Figure 16 provides insight for the rate at which each simulation expends propellant mass relative to the reconstruction. Computing the error profiles shown in Figure 16 required the simulated results to be synchronized in time with the BET. Thus, for simplicity, the simulated results and the BET were all linearly interpolated to have matching data rates.

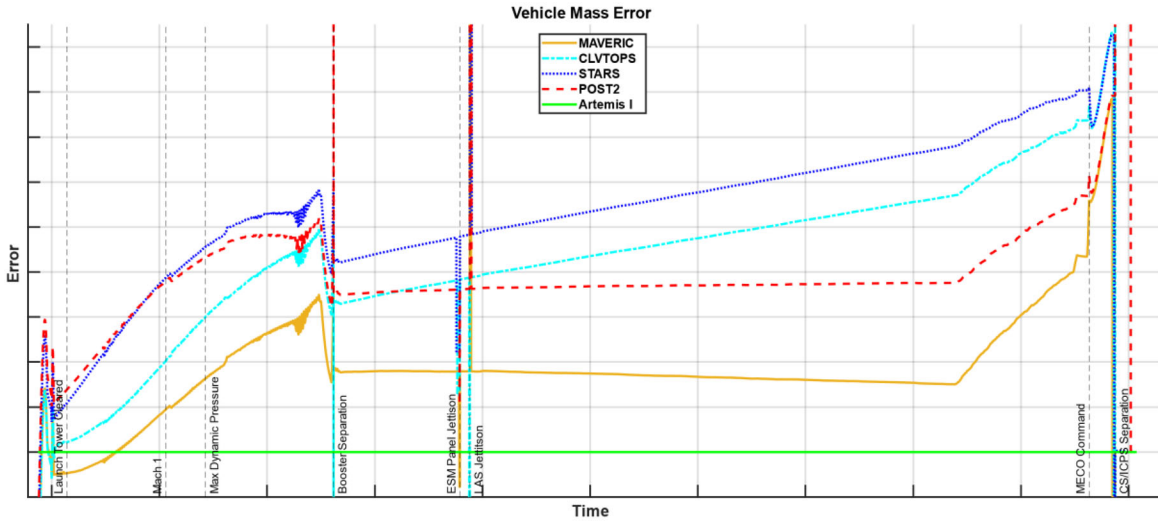

Figure 16. Simulated Vehicle Mass Error Over Time

Prior to SRB separation, the simulated propellant mass flow rate was slower than the reconstruction due to their increasing error. Additionally, MAVERIC was the only simulation with less mass than the reconstruction after the launch tower was cleared. However, because MAVERIC and CLVTOPS began with the same vehicle mass, as seen in Figure 15, MAVERIC must therefore be expending more propellant mass than CLVTOPS prior to launch tower clearance.

After SRB separation, STARS and CLVTOPS had approximately the same mass flow rate. Additionally, during this time it also appeared that the core stages for these two simulations were not expending propellant mass fast enough compared to the reconstruction given the linear increase in error between LAS jettison and the Core Stage throttle down prior to MECO. In contrast, POST2 and MAVERIC mass errors were near constant after SRB separation until the core engines began to throttle down prior to MECO. Therefore, these simulations were expending propellant mass at approximately the same rate as the reconstruction during this segment of the trajectory. Note that error spikes located at the separation event boundaries are generally attributed to interpolation error.

Finally, it was expected that the offsets in initial vehicle mass from Figure 15 combined with different propellant mass consumption rates in Figure 16 were compounding throughout the trajectory and were likely a primary contributor of the observed differences in altitude mid-trajectory in Figure 7. Postflight adjustments to the core engine performance, and thereby the propellant mass consumption rate, were typically implemented as multiplicative factors and/or additive bias to better match BET results (i.e., the model itself was not updated).

Tail Wags Dog Force & Moment Contribution

Tail wags dog (TWD) forces and moments are plotted in Figures 17 and 18, respectively. TWD forces and moments are reaction forces and moments due to nozzle dynamics that are coupled with rigid and flexible bodies. Figures 17 and 18 show that large TWD forces and moments were predicted by MAVERIC. After this analysis was performed, it was determined that the MAVERIC simulation was inadvertently reporting different simulation variable(s) for TWD forces and moments, and this was corrected. Reconstructed TWD data was not available for this analysis thus, Figure 17 and Figure 18 are purely simulation comparisons that illustrate the value of comparing simulations against each other to achieve analysis goals rather than only comparing simulation results against the BET.

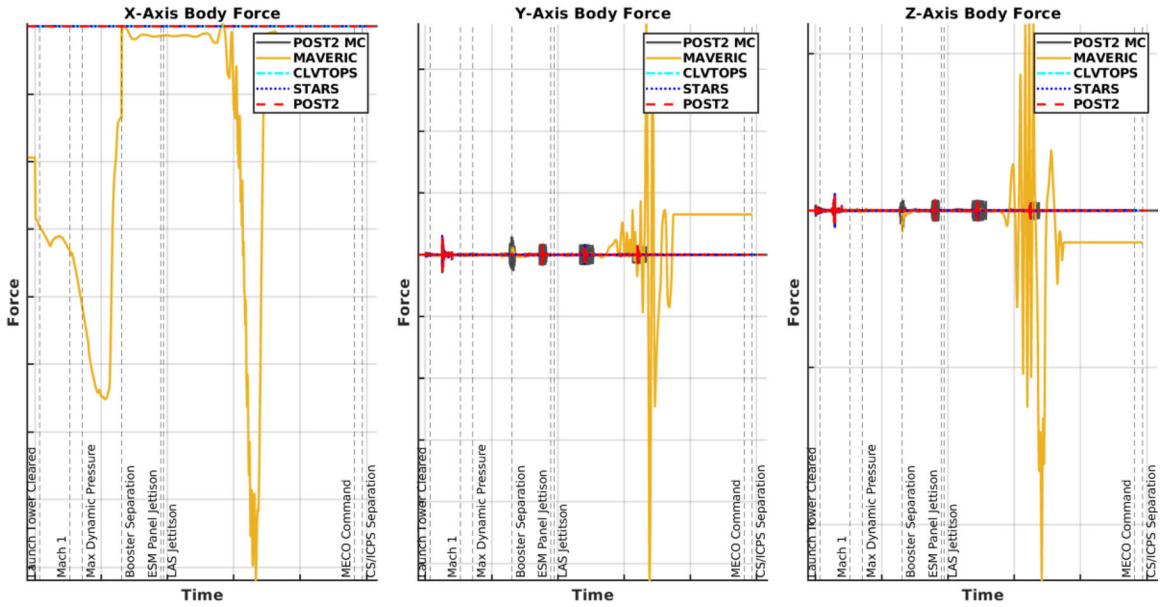

Figure 17. Simulated TWD Forces

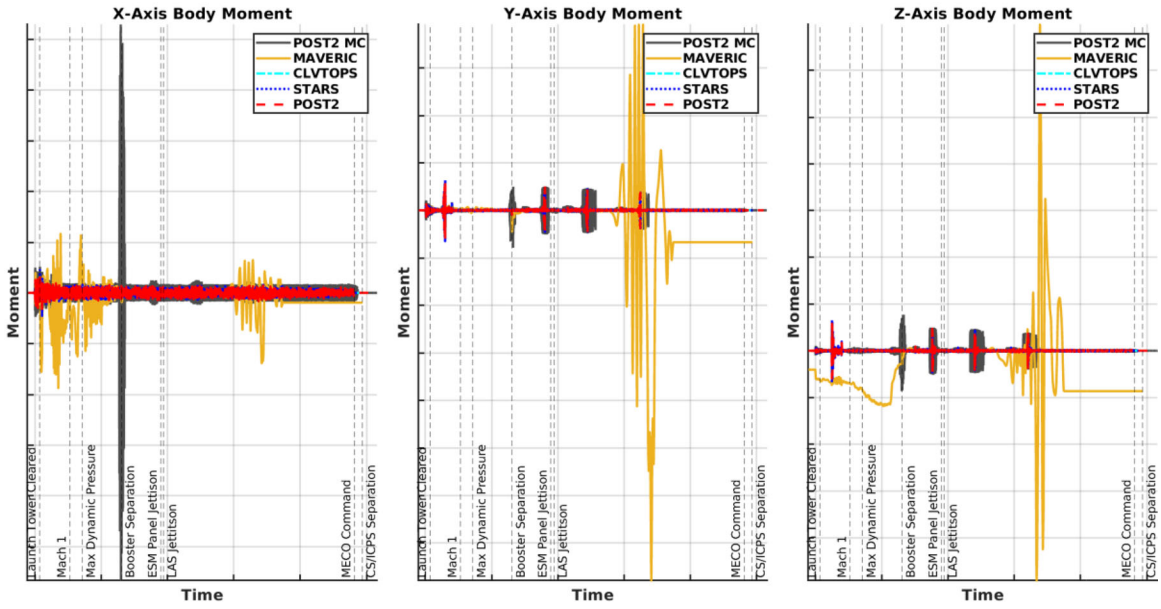

Figure 18. Simulated TWD Moments

Interim Cryogenic Propulsion Stage Slosh

Figure 19 plots the ICPS propellant slosh forces in the Liquid Oxygen (LOX) tank. It was observed that the POST2 x-axis LOX slosh force did not align with the other simulations. Additionally, while there appears to be a better agreement in the y and z-axes, there still appears to be some differences in the POST2 results here as well. Note that reconstructed slosh data was not available for this comparison.

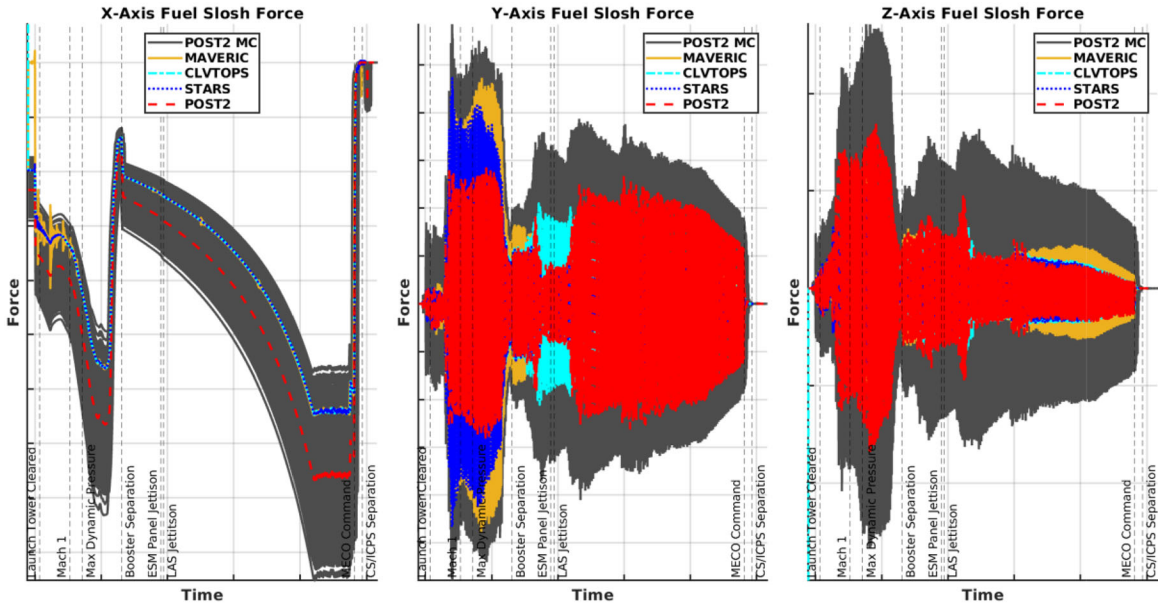

Figure 19. ICPS LOX Slosh Force

In addition to the differences observed in Figure 19, Figure 20 shows that the fill height and the propellant sloshing mass for POST2 is again an outlier compared to the other simulations. Figure 20 shows that the tank fill height and fuel sloshing mass are constant throughout the trajectory, which indicates that the ICPS does not perform a burn during this portion of the ascent trajectory. This comparative effort revealed that the POST2 team had implemented a newer ICPS slosh data delivery, which resulted in a different tank state in Figure 20 and thereby different slosh dynamics in Figure 19. The ICPS slosh data used by the other simulations was not considered out-of-date at the time this analysis was completed rather, POST2 had implemented a more mature model. As a result, the POST2 simulation maintained this slosh data delivery.

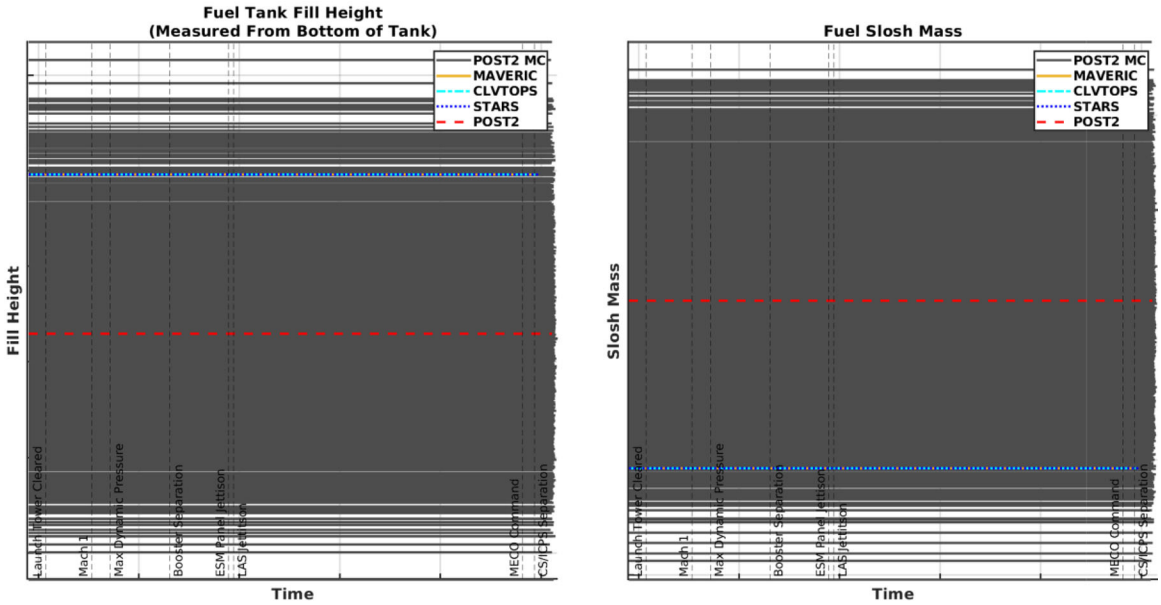

Figure 20. ICPS LOX Tank Fill Height and LOX Sloshing Mass

CONCLUSIONS

The simulations were generally in close agreement with each other and the Artemis I BET datasets. Minor simulation errors and anomalies were corrected and areas for improvement regarding existing models was documented. The results presented in this paper focus on the most significant differences observed between postflight simulated results when compared against the Artemis I BET whereas the complete analysis compared a total of 277 discrete simulation variables. Overall, these results validate each tool's simulation capabilities and provide a benchmark regarding simulation accuracy which support future Artemis analyses and missions.

Future Work – Preparing for Future Space Launch System Flights & Lessons Learned

In addition to preparing preflight simulation capabilities for future Artemis Missions, this analysis provided the opportunity to consider other metrics and analytical methods that will be useful for future postflight analyses. Recall that this analysis was primarily a qualitative effort to confirm that the simulated nominal results closely aligned with the BET and that the BET was bounded by the Monte Carlo results. The qualitative nature of this analysis was driven by a variety of different factors.

At the start of this analysis, implementing a requirement to quantify and determine simulation accuracy was considered but was ultimately disregarded for several reasons. It was observed that postflight simulation accuracy was primarily dependent on the amount of DOL data available. Therefore, it was considered that the simulation results could theoretically always be improved with the addition of more DOL data. Since the Artemis I mission was already complete it had become easily subjective to simply pick a requirement that yielded favorable results rather than one that definitively confirmed simulation accuracy.

Determining a consistent method of quantitative comparison that was sufficient for the extensive list of variables considered also proved difficult, which made defining a requirement infeasible. Simply computing the time history of error between the BET and the simulation results, such as in Figure 16, is a predictable place to begin such an analysis and though these error plots can provide meaningful comparisons in many cases, they also invited other computational challenges. Recall that Figure 16 required datasets to be linearly interpolated to the same data rate such that each dataset contained the same number of datapoints. This step introduces some error into the comparison especially around separation event boundaries, which are discontinuities. Datasets that do not report separation events at the exact same time step can potentially generate extremely large errors. For example, although not visible the error spikes present in Figure 16 extend far beyond the figure boundaries. Such error spikes are misleading at first and must be addressed on a case-by-case basis, which is cumbersome due to the amount of data considered in this analysis. Also, because so many different simulation variables were compared against each other, the magnitude of error was highly inconsistent, and it became unclear what was a significant or insignificant amount of error. Error computations were also found to be a poor comparison for simulation variables that were highly oscillatory. Large errors were generated for such variables when datasets were out of phase, especially for variables that oscillated about zero with their frequent change in sign. Additionally, percent difference computations encountered further issues with these types of oscillatory variables due to situations when the limit of the denominator approached zero, which drove deceptively large percent differences. Alternatively, percent error computations could alleviate some of these issues described but, not the error spike issue at separation event boundaries.

Despite some of these computational challenges, future postflight analyses will likely include more error and percent error computations, but for select variables of interest. Error analyses

might also evaluate the average or weighted average error over time for the entire trajectory as well as different phases of flight to mitigate the presence of error spikes at separation event boundaries. Additionally, rather than interpolating all datasets to the same number of datapoints, future analyses will likely only interpolate the simulated results to avoid postprocessing the BET to reduce error in the analysis. Also, rather than observing that the BET is simply bounded by the Monte Carlo, it would likely be more useful to evaluate if the BET is bounded by the three, two, or one-sigma Monte Carlo bounds. Comparing the BET to the Monte Carlo results in this manner could help quantify "boundedness" of the BET, which could potentially be a useful and generic metric across all simulation variables.

Finally, it could be useful to observe and quantify how much postflight models have changed from preflight models. Thus, a future Artemis II postflight reconciliation would likely involve a greater effort to report how much DOL simulation inputs have changed from their preflight models and would also evaluate how much the simulation results improve from preflight predictions to a postflight simulation.

ACKNOWLEDGEMENTS

- Evan Roelke for his contribution to modeling and simulation for Space Launch System in POST2 and for feedback with this analysis.
- Dan Yuchnovicz for his contribution to documenting the Artemis I post-flight results in the NESC Final Report.
- Ben Burger, Joey Harlin, Thomas Park, Frank Willis, Nick Hoen, and the rest of the SLSP for their collaboration and feedback involved with this analysis, for generating their respective DOL simulations, and for generating the many postflight data products that collectively make up the BET for this postflight comparison effort that are listed in Table 2 and Appendix A.
- The NESC for supporting this work under NESC Assessment TI-12-00766, "Exploration Systems Independent Modeling and Simulation."

APPENDIX A: SUMMARY OF DATA PRODUCTS

Table 4. Summary of Data Products

Data Product Description	Contents
MAVERIC Nominal Trajectory	Artemis I DOL Simulated Results
CLVTOPS Nominal Trajectory	Artemis I DOL Simulated Results
STARS Nominal Trajectory	Artemis I DOL Simulated Results
POST2 Nominal Trajectory	Artemis I DOL Simulated Results
POST2 Dispersed Trajectories	Artemis I DOL Simulated Monte Carlo Results
Artemis I Trajectory Reconstruction	Artemis I Trajectory Parameters (BET)
Artemis I Aerodynamic Reconstruction	Artemis I Aerodynamic Coefficients (BET) Artemis I Base Force Profile (BET & DOL Inputs)

Artemis I Booster Reconstruction	Artemis I Booster Performance (BET & DOL Inputs)
Artemis I Telemetry Measurements	Artemis I Raw Flight Data (BET)
Artemis I Event Times	Trajectory Event Timestamps (BET)
Artemis I Atmospheric Profile	DOL Atmospheric Conditions (BET & DOL Inputs)
Artemis I Mass Properties Reconstruction	Artemis I Mass Properties Time-History (BET)
Artemis I Reconstructed Initial Mass Properties	Artemis I Initial Mass Properties (DOL Inputs)
Artemis I Core Engine Performance Adjustments	Artemis I Core Engine Performance Bias & Factors
Artemis I DOL GN&C	Artemis I DOL GN&C Inputs & Commands (DOL Input)

REFERENCES

[1] Action, C.H.: "Ancillary Data Services of NASA's Navigation and Ancillary Information Facility;" Planetary and Space Science, Vol. 44, No 1, pp. 65-70, 1996. DOI 10.1016/0032-0633(95)00107-7

[2] Burger, B.S.; Addona, C; Diedrich B.; Harlin, W.J.; McDonough P.; Muscha Z.; Sells R.; and Tyler D.: "Space Launch System Liftoff and Separation Dynamics Analysis Chain Tool," AIAA Paper 2021-0822, 2021. DOI 10.2514/6.2021-0822

[3] Gilbert, M. G., "Purpose, Principles and Challenges of the NASA Engineering and Safety Center", 8th IAASS Conference "Safety First, Safety for All," May 18-20, 2016, Melbourne, FL.

[4] Hough, S.L.; Compton, J.D.; Hannan, M.R.; and Brandon, J.; "Time Domain Tool Validation Using Ares I-X Flight Data," 58th JANNAF Propulsion Meeting, JANNAF, April 2011; also Paper 1830.

[5] McCarter, J.W.: "Simulating Flights of Future Launch Vehicles and Spacecraft", NASA Tech Briefs, 2007. Retrieved January 7, 2025 from https://www.techbriefs.com/component/content/article/1182.

[6] Tartabini, P.; Starr, B.; Shidner, J.; Lugo, R.; Tackett, B.; Lee E.; Angster S.; Pamadi B.; Covell P.; and VanZwieten, T.: "Modeling, Simulation, and Visualization Environment to Support Independent Verification and Validation of Artemis I Separation Events," ESA GNC-ICATT Paper, 2023. DOI 10.5270

[7] Tartabini P.; VanZwieten Cook, T.; Starr B.; Lugo R.; Lee E.; Fleck J.; Ernst Z.; Pamadi B.; Covell P.; "Independent Verification and Validation of Artemis 1 Separation Events," AAS-25-123, 2025

[8] Wilson, T.; VanZwieten, T.; Yuchnovicz, D.; Lugo, R.; Burke, L.; Fleck, J.; Pamadi, B.; Tartabini, P.; Koehler, H.; Lee, E; Starr, B.; "NASA Engineering and Safety Center Technical Assessment Report Artemis I Post-Flight Analysis and Interim Cryogenic Propulsion (ICPS) Disposal Volume 1," NESC-RP-12-00766, Vol. 1, May 30, 2024